

## Article

# Simple Design Solution for Harsh Operating Conditions: Redesign of Conveyor Transfer Station with Reverse Engineering and DEM Simulations

Błażej Doroszuk <sup>\*</sup> , Robert Król  and Jarosław Wajs 

Faculty of Geoengineering, Mining and Geology, Wrocław University of Science and Technology, Na Grobli 15, 50-421 Wrocław, Poland; robert.krol@pwr.edu.pl (R.K.); jaroslaw.wajs@pwr.edu.pl (J.W.)

\* Correspondence: blazej.doroszuk@pwr.edu.pl

**Abstract:** This paper addresses the problem of conveyor transfer station design in harsh operating conditions, aiming to identify and eliminate a failure phenomenon which interrupts aggregate supply. The analyzed transfer station is located in a Polish granite quarry. The study employs laser scanning and reverse engineering methods to map the existing transfer station and its geometry. Next, a discrete element method (DEM) model of granite aggregate has been created and used for simulating current operating conditions. The arch formation has been identified as the main reason for breakdowns. Alternative design solutions for transfer stations were tested in DEM simulations. The most uncomplicated design for manufacturing incorporated an impact plate, and a straight chute has been selected as the best solution. The study also involved identifying areas of the new station most exposed to wear phenomena. A new transfer point was implemented in the quarry and resolved the problem of blockages.

**Keywords:** conveyor belts; transfer station; DEM simulation; reverse engineering



**Citation:** Doroszuk, B.; Król, R.; Wajs, J. Simple Design Solution for Harsh Operating Conditions: Redesign of Conveyor Transfer Station with Reverse Engineering and DEM Simulations. *Energies* **2021**, *14*, 4008. <https://doi.org/10.3390/en14134008>

Academic Editors: Daniela Marasova, Monika Hardygora and Mirosław Bajda

Received: 25 May 2021  
Accepted: 28 June 2021  
Published: 2 July 2021

**Publisher's Note:** MDPI stays neutral with regard to jurisdictional claims in published maps and institutional affiliations.



**Copyright:** © 2021 by the authors. Licensee MDPI, Basel, Switzerland. This article is an open access article distributed under the terms and conditions of the Creative Commons Attribution (CC BY) license (<https://creativecommons.org/licenses/by/4.0/>).

## 1. Introduction

Transfer points are critical components of large belt conveyor systems in the mining industry, and their proper functioning is essential for the proper performance of other elements. Breakdowns caused by transfer point failures contribute to enormous energy losses due to downtime in the supply of the transported material and to sub-optimal use of available technological resources [1]. Improper design of the transfer station also causes increased resistance at the loading point of the conveyor belt [2], thus increasing the energy demand of the drive system for a particular conveyor. When analyzing the energy consumption of the belt conveyor system as a whole, the impact of transfer station design and its optimization cannot be ignored. An optimally designed transfer point also reduces potential damage to the receiving belt caused by falling solids if these are of a size that can damage the conveyor belt [3]. Researchers have extensively explored the topic of the potential damage to the belt from falling objects [4–6]. Therefore, a properly designed station decreases the costs of conveyor belt replacement.

Many previous generation industrial plants, including mines, have transfer points that were designed following a rule of thumb [7]. They often do not have detailed documentation, and after each failure, they were modified by trial and error. Additional metal sheets are often welded to the structure in order to prevent the material from spilling or to solidify the areas most exposed to abrasion. On occasion, some elements are cut to make more space for the material stream after a blockage. Poorly designed transfer points are often repaired using only makeshift measures, and after a critical failure, the entire construction has to be redesigned. The best solution would be to replace the old elements entirely with new versions, designed according to the latest standards. However, the complete removal of a structure and the construction of a new one is a very expensive task, and not every

plant can afford such an undertaking. Therefore, it is economically justified to cut out only some of the unnecessary elements of the old transfer station and fit new ones into the existing structure. Reverse engineering methods prove very useful for designs that do not have sufficient documentation. These methods allow mapping the geometry of the current equipment digitally, in the form of CAD models. Engineers can easily modify such models and validate them with simulation methods.

For years, continuum-based analytical methods were the only tools available to transfer station designers [8]. Several studies have made comparisons between continuum-based analysis and computational methods [8,9]. When designing transfer stations operating in difficult conditions, the most frequently used method is the discrete element method (DEM), one of the most important simulation techniques developed for the analysis of particulate systems [10]. The method has gained popularity with the increase of computing power, and the first industrial applications date back to the early 1990s [11]. In 1994, Nordell successfully predicted that engineers would extensively use this method for transfer station design [12]. DEM enables simulations of the behavior of bulk materials. The simulations are on the level of separate material particles and their interactions with each other and with the geometry understood as boundaries for particle movement. With this method, it is possible to map specific conditions under which failures occur in existing transfer points and conduct an in-depth analysis in order to understand the mechanism behind, e.g., a blockage in the transfer point.

This paper will discuss an optimization process performed for an existing transfer station in a quarry. The discharge connects two conveyors at an acute angle, where the first conveyor is wider than the second conveyor, with the latter additionally being sharply sloped. Further, in the current situation and under specific conditions, the risk of blockage highly increases. The latest works on DEM application in designing and analyzing the efficiency of transfer stations refer to stations with a known geometry [9,13,14]. A novelty in this work is the combination of laser scanning to map an existing transfer point and then the use of real geometry in DEM simulations for further analysis.

## 2. Case Study

The optimized transfer station is located in the “Graniczna” quarry in the Dolnośląskie Voivodeship in Poland. The quarry extracts granite and processes it into aggregate. The discharge connects two belt conveyors, WD-1 (feeding) (Figure 1a) and B-1 (receiving) (Figure 1b).



**Figure 1.** Conveyors connected by analyzed transfer station: (a) feeding conveyor belt WD-1 and (b) receiving conveyor belt B-1.

The WD-1 conveyor has a 1.2 m wide belt (Cobra DX FLEXAMID 3150/1 1200 10 + 4), is inclined at an angle of  $7.39^\circ$ , and has a velocity of 1.63 m/s, while the B-1 conveyor has a 1 m wide belt (Wolbrom 1000 EP 800 4 4 + 2) inclined at an angle of  $16.4^\circ$ , and has the velocity of 1.85 m/s. The DX FLEXAMID belt is a 1-ply belt with textile carcass and rubber covers, and

the Wolbrom belt is a 4-ply polyamide-polyester belt. The temporary value of the capacity recorded on the crusher feeding the WD-1 reaches almost 900 Mg/h (Figure 2). The crushed product fed to conveyor WD-1 has grain composition, as presented in Figure 3.

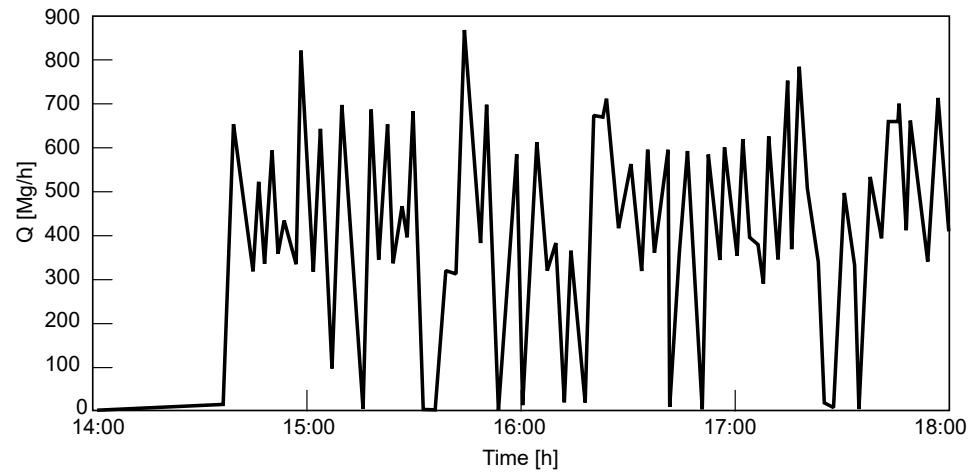


Figure 2. Capacity of the crusher feeding the WD-1 conveyor.

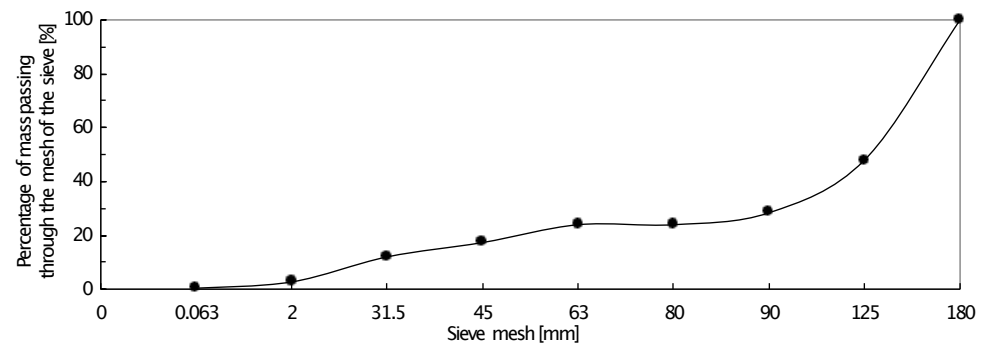
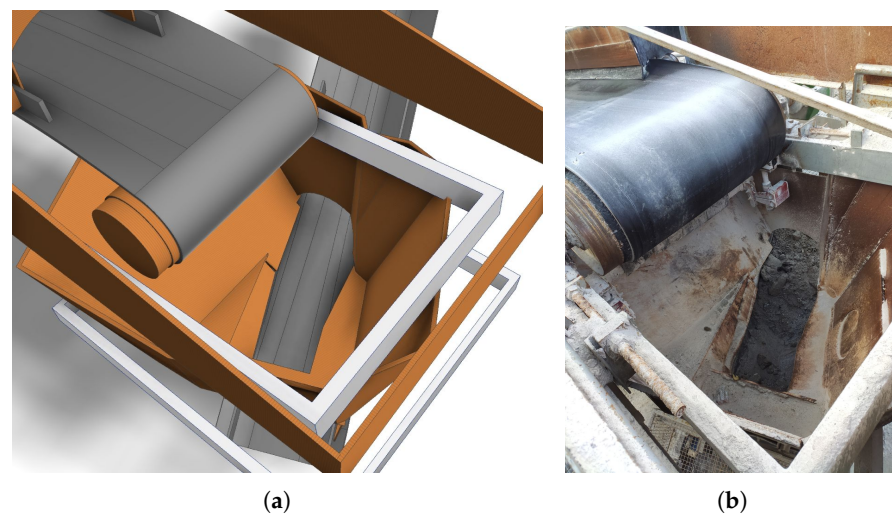


Figure 3. Cumulative particle size distribution.

The angle between the conveyors is  $23.6^\circ$ , and the height difference is about 2 m. It means that transfer station WD-1/B-1 has to change the direction, in a very limited space, of the aggregate stream by  $156.4^\circ$  in the horizontal plane.

The current transfer station is hard to classify as a specific type of construction, but it has some “rock box” features. There are shelves inside (Figure 4) that allow for material retention. The stream of granite does not directly hit the elements of the station, it only loses energy on the piled aggregate. Then, the material is discharged onto the receiving conveyor. The construction has been modified many times, as evidenced by numerous irregular welded plates and a cut-out in the front wall, increasing the space for the aggregate stream. However, despite the modifications, blockages still occur under unfavorable working conditions, i.e., during bad weather, at very high temporary capacity, and also in the case of larger rocks.

The requirement for the modification process was to create a simple-to-build transfer point that would fit into the current main structure of the transfer point. The engineers in the quarry expressed a preference for flat surfaces to be included in the new design.



**Figure 4.** The inside of the transfer station: (a) CAD model and (b) existing station.

### 3. Materials and Methods

#### 3.1. Laser Scanning

The literature shows that terrestrial laser scanning is commonly applied in mining areas and allows rapid data acquisition for developing 3D mine models [15], ensuring slope stability [16], and detecting changes based on two TLS point clouds [17]. The application of TLS data, as presented in [18], proves the usefulness of 3D point cloud data for structural health monitoring (SHM) of constructed objects.

LiDAR data from a laser scanner allow the monitoring of long-range engineering objects (e.g., a steel trestle bridge) [19] and the modeling of mining shaft deformations [20]. The current status of the development trends in, and the potential for, TLS application in mining areas were described in detail in [21]. Based on active sensors, LiDAR techniques help to detect the shape of the object, which can be transported by the conveyor belt [22] and detect the damage [23]. In the present case study, the acquired point cloud allowed the building of a 3D BIM model in order to reconstruct the shape of the analyzed equipment (transfer station).

The LiDAR data were acquired following the terrestrial approach (TLS) with the multi-station acquisition, significantly reducing the number of potential occlusions. The 3D point cloud was obtained from the Riegl V400i terrestrial laser scanner (Figure 5a). The point cloud post-processing involved full multi-station adjustment with high internal and external quality of the geo-referenced final point cloud. The resulting post-processed scans represent the full metric point cloud, which can be used to identify, design, and measure objects in a metric 3D model (Figure 5b). The product of the 3D laser scanning procedure provides excellent data for the 3D modeling of mining objects in the BIM (building information modeling) technology. The final point cloud provides information about the intensity, amplitude, and, optionally, RGB values for each point in the point cloud. TLS measurements allow the reverse engineering method to be employed for future CAD modeling of the analyzed transfer stations based on the original geometry from the TLS point cloud.

#### 3.2. Theoretical Capacity of the Conveyor Belts

Material flow through curved or straight chutes can be categorized as “fast” or “slow” [24]. When the chute works under fast flow conditions, the material stream thickness varies along the chute, with minimum thickness near the area of maximum stream velocity [24]. Solutions providing fast flow conditions at the maximum capacity of the feeding belt will be tested as part of further research works. Belt capacity should correspond to peaks of material volumetric discharge from the feeding point [25]. In the analyzed case, the material supplied by trucks and loaders to the jaw crusher is fed to the conveyor. The nominal



capacity of the conveyors was determined from theoretical cross-sections and from belt cross-sections obtained in the scanning procedure (Figure 6). The theoretical cross-section was calculated from the dependencies described in [26]. The width of the supplied material was projected from the theoretical cross-sections onto the actual cross-sections of the belts, and the material surface area was drawn using the same angles of repose as above.

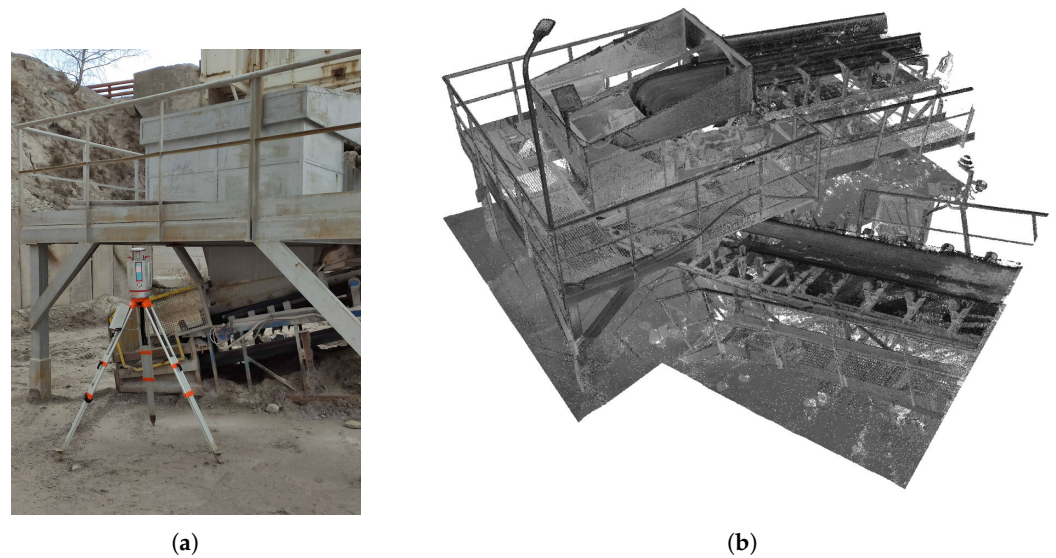


Figure 5. Laser scanning: (a) Riegl V400i scanner and (b) point cloud of transfer station.

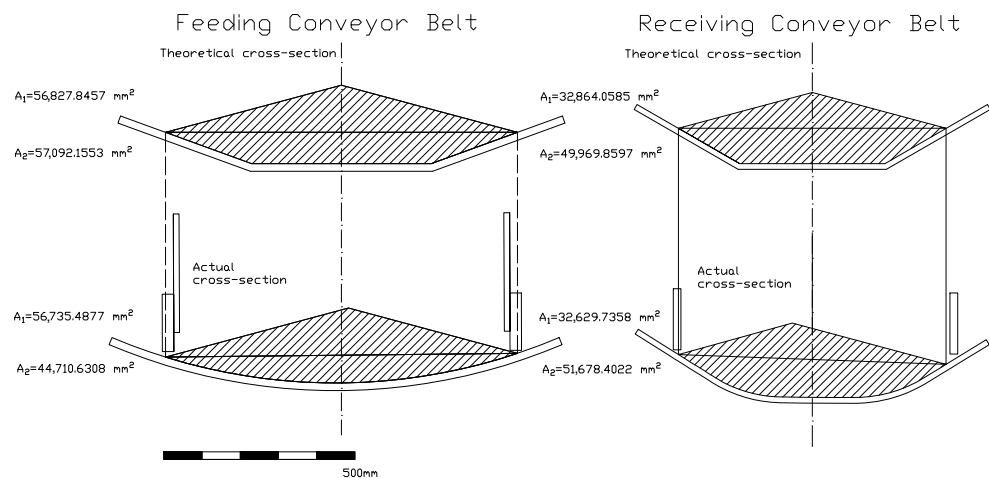


Figure 6. Cross-section of loaded conveyor belts.

It is worth noting that when scanned, the belts were empty, so the actual capacity of the conveyors will not be less than the capacity determined for the existing cross-sections of the empty belt. Still, it should not be greater than the nominal capacity determined analytically. As a result, the capacity remains within the following ranges:

- WD-1: 837–1123 Mg/s
- B-1: 692–751 Mg/s

Conveyor B-1 has a nominal capacity smaller than the maximum capacity of the crusher that feeds conveyor WD-1, which may lead to problems.

### 3.3. CAD Model

Using CAD tools, the solids were adjusted to the point cloud. The mapping was limited to only those elements of the geometry of the transfer station which may come into direct contact with the bulk material and the elements limiting the construction space.

Knowledge of space limitations is necessary to fit a new transfer station into the existing main construction. The geometry has been simplified and is represented by flat faces (Figure 7).

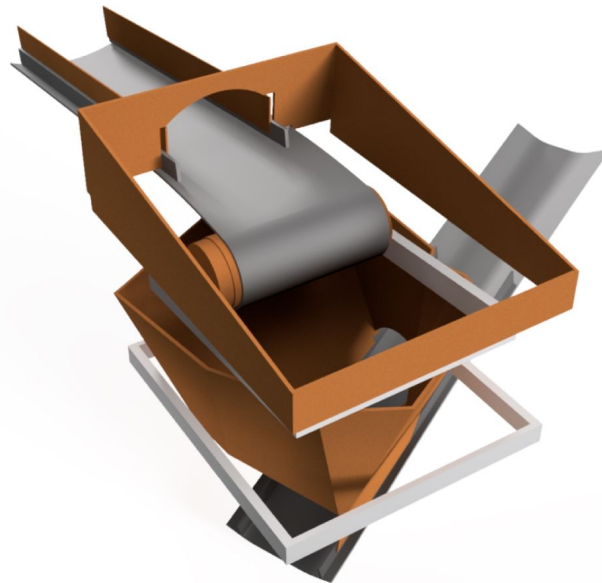


**Figure 7.** CAD model of the transfer station.

#### 3.4. DEM Model

The importance of selecting proper model parameters was demonstrated in [27]. In the publication, granite aggregate samples (16–22 mm) and several larger granite rocks were collected from a quarry. Three cylindrical specimens with a diameter of 43 mm and a height of 86 mm were cut from the larger rocks, which were then tested by the uniaxial compression test. The tested granite had an average density of  $2612 \text{ kg/m}^3$ , a Poisson's ratio of 0.11, and a Young's modulus of 18.4 GPa. The friction coefficient of granite against steel and the conveyor belt rubber was also investigated using an inclined plane, obtaining average values of 0.46 and 0.76, respectively.

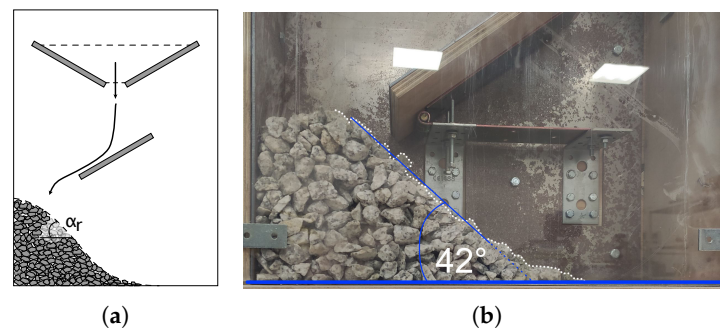
The aggregate particles were mapped as four conglomerates of spheres, consisting of 4 to 7 spheres to reflect the irregular shape of the particles. Parameters that cannot be measured directly were calibrated by imitating the material flow in the calibration box (Figure 8a). The calibration aimed to achieve a set of DEM parameters that provide a simulation of the flowing material in approximation to the actual conditions with respect to the time flow and the granite angle of repose. The edge of the piled-up aggregate was redrawn on the photo manually, and then the trend line was matched with the dots, as shown in the figure below (Figure 8b). The calibration process was similar to that in the previous works [28,29]. Researchers [30] have shown that obtaining correspondence in two different parameters during an experimental simulation may be sufficient to obtain a unique set of parameters, allowing the behavior of bulk material to be adequately simulated. The obtained parameters from calibration are presented in Table 1 and the material parameters used during calibration and simulations are presented in Table 2. Young's modulus of the Granite was reduced 2000 times, to 9.2 MPa, so the simulation time-step time dependent on that parameter could be longer. The value of Young's modulus was chosen as minimal as possible, which provided the same results in simulations as the original but drastically reduced the computing time. Simulations were performed with the time-step equal to 0.00024 s.

**Table 1.** Calibrated parameters.

Coefficient of	Granite-Granite	Granite-Rubber	Granite-Steel
Restitution	0.2	0.3	0.2
Static Friction	0.7	0.53	0.32
Rolling Friction	0.05	0.01	0.01

**Table 2.** Material parameters.

Parameter	Granite	Rubber	Steel
Density (kg/m <sup>3</sup> )	2610	1100	7800
Young's Modulus (MPa)	18,400 (9.2)	8.69	200,000
Poisson's Ratio (-)	0.11	0.499	0.3

**Figure 8.** Calibration: (a) scheme of the calibration box and (b) granite angle of repose.

The grain composition of the simulated material was adjusted (based on data shown in Figure 3) using normal distribution, with an average of 110 mm and a standard deviation of 40 mm, so that the mean grains of the simulated and of the actual material were similar. Solids smaller than 50 mm were rejected in the simulation.

### 3.5. DEM Simulations

The simulations were carried out for normal (300 Mg/h) and extreme conditions (900 Mg/h), as well as for humidity causing reduced friction coefficients and for increased number of solids of up to 300 mm in diameter. During one time step, the maximum generated amount of particles was approximately 1500, which corresponds to about 9000 total spheres building all particles. Due to a small percentage of the dust fraction, cohesive interactions were neglected. Research shows that rubber friction for wet surfaces is 20–30% smaller than for corresponding dry surfaces [31]. A 30% reduction in particle-geometry friction was assumed when humidity was taken into account for further analysis. The first simulations were carried out for a transfer station according to the original design, and subsequent simulations for alternative considered solutions. In the EDEM Software simulation environment, the motion called “conveyor translation” was assigned to conveyor belt geometries. Conveyor translation makes particles in the contact of the belt surface move with the belt velocity and direction. The belt in the simulation does not move, but bulk material that comes into interaction with the belt surface moves like on the real conveyor belt.

## 4. Results of Numerical Analyses

### 4.1. Mapping the Work of the Transfer Station

The performance of the transfer station according to the original design was mapped for the simulated grain composition and for a capacity of 300 Mg/h. No disturbing phenomena were observed in the case of these performance settings. The material was placed on a shelf inside the station of the original solution, and then it fell onto the receiving belt.

Several simulations were performed in order to identify the failure mechanism. They considered factors such as the capacity increased to 900 Mg/h (Figure 9a), a greater number of solids having a diameter of up to 300 mm, and increased humidity (lower friction coefficients against steel and rubber).

It has been observed that the performance increase itself does not cause failures. However, with other factors included, the phenomenon of “arch” formation was observed (Figure 9b) in the transfer station discharge opening. When larger particles account for 30 percent of the excavated material, the arch may be formed at a temporary capacity of 800 Mg/h. However, with moisture and large solids, the phenomenon can be observed even at a temporary capacity of 600 Mg/h.



**Figure 9.** Observed failure: (a) simulation of material flow through the transfer station at a capacity of 900 Mg/h and (b) the observed arch formation.

The discharge opening of the current transfer station is similar to the discharge of the hopper. In the case of the hopper, the space for mass flow must be sufficient to prevent the formation of the cohesive/mechanical arch. Research [32] suggests that the opening width should be at least four times the maximum particle dimension. Under the analyzed conditions, this would mean that the opening should be 1200 mm wide, i.e., 200 mm more than the width of the receiving conveyor belt.

#### 4.2. Alternative Designs

Possible modifications to the present transfer station were tested under the worst-case conditions. A minimal improvement was achieved by designing a new rock box, but it did not meet the requirements (it was not failure-free in the worst analyzed conditions). Such a design solution does not change the method behind the transfer station discharge, which is still similar to unloading the hopper, the mass-flow opening of which should be wider, as mentioned previously. Modifications of the existing geometry were limited by the main steel frame of the transfer station and its location in the transportation system.

However, numerous research works have already demonstrated a potential for the use of curved elements in transfer stations. They provide an easy solution for redirecting the stream of material [2]. Curved chutes have many advantages: (a) reducing the need for belt covers of a significant thickness, (b) no need for large steel cord filament diameters to resist impacts, and (c) spillage prevention [12]. Straight chutes are easier to manufacture and have favorable material streamflow characteristics [24].

Hence, the idea of the hood and spoon transfer operation was tested. This type of design provided satisfactory results. The station consists of two profiled elements redirecting the stream of material in the desired direction. However, it is a complicated structure that requires bent parts and is currently not considered by the plant staff for the new design. The main advantage of the construction is that it feeds the aggregate stream continuously, and it does not accumulate any material that could later cause blockage, as is the case with the present construction. Therefore, it was decided to use the idea of continuous feeding with the most straightforward possible structure. A satisfactory effect was obtained using a structure consisting of two main steel elements: an inclined impact plate, which redirects the stream of material downwards, and then a straight chute, along



which the granite slides onto the receiving belt (Figure 10a). As shown in Figure 10b, the area in which the material accelerates to reach the belt speed is very short.

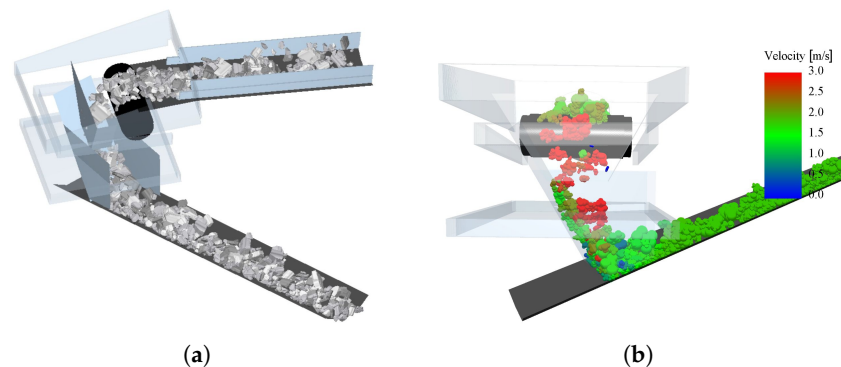


**Figure 10.** Simulation of material flow through the new transfer station at a capacity of 900 Mg/h: (a) visualization and (b) velocity of the particles.

The current station has been compared with the design, in which the steel impact plate is 770 mm from the feeding conveyor head pulley axis, and the chute is set at an angle of  $60^\circ$ . The influence of the impact plate inclination by  $10^\circ$  and a change in the inclination of the bottom part of the chute to  $45^\circ$  (an angle slightly greater than the angle of repose of natural granite) were also investigated. The impact plate was placed in such a position that the material was redirected into the center of the chute. The angles of the chute were limited by the available space.

Comparisons also involved the distribution of cumulative normal energy lost by the material stream on the belt during collisions. The surface that receives impacts in the current station is concentrated in the center of the belt, which may cause uneven wear (Figure 11).

The total normal energy that the belt acquires during the simulation for each of the analyzed variants of the transfer station is shown in Figure 12. The total normal energy was exported for the successive time steps of the simulation, with a constant time interval. Then, using linear regression, the trend lines were fitted to the data. It shows that by using a  $45^\circ$  chute, it is possible to reduce the energy that the material loses on the receiving belt by more than 10 percent compared to the currently lost energy.

The design of an angular discharge is obligatory so that the material is evenly fed on the belt, as an uneven placement of the aggregate stream may cause misalignment [33]. The use of the chute ensures even distribution of the material along the width of the belt.

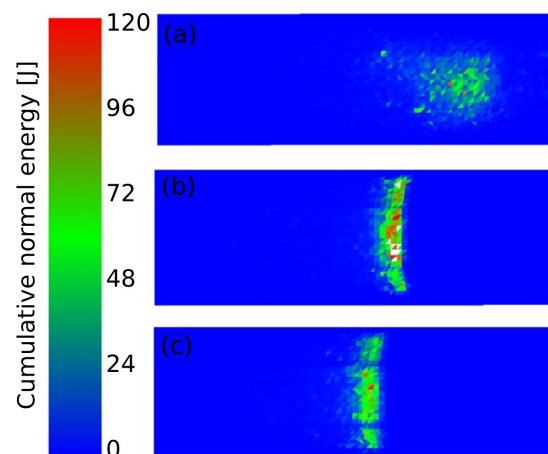


**Figure 11.** Distribution of the cumulative normal energy transferred by the material stream to the receiving belt after 60 s of simulation: (a) current transfer station, (b)  $60^\circ$  chute, and (c)  $45^\circ$  chute.

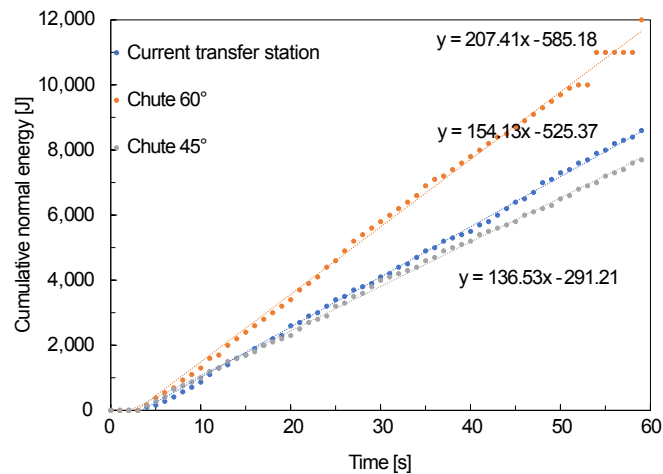


**Figure 12.** Total cumulative normal energy absorbed by the belt during collisions with the material for a capacity of 300 Mg/h.

#### 4.3. Determination of the Elements Most Exposed to Wear

In addition to the energy loss due to collisions with the receiving belt, the material also loses energy as it slides down the chute. Studies have shown that under thin-stream accelerated flow, the energy losses are approximately: 82% due to sliding along the chute bottom, 9% due to sliding against sidewalls, and 9% due to inter-granular friction [34].

During the simulation, it is possible to analyze many different parameters resulting from the interaction of the bulk material with the elements of the geometry. The energy transferred to the geometry depends on the mass and velocity of the particles during the collisions. The tangential and normal energies that act on the impact plate were investigated when this was mounted vertically and inclined by  $10^\circ$ , and on the chute in the variant in which the entire chute was inclined at an angle of  $60^\circ$  and in which the bottom part of the chute was inclined at an angle of  $45^\circ$ . The inclination of the impact plate by  $10^\circ$  was observed to have a positive effect on reducing the normal energy loss by the impacting material stream, which helps to reduce the noise and the damage to the element. The tilt also causes a more even distribution of the tangential energy (Figure 13) (the energy responsible for the abrasions on the surface). The  $45^\circ$  inclination angle of the chute can provide more even distribution of the tangential energy (Figure 14).

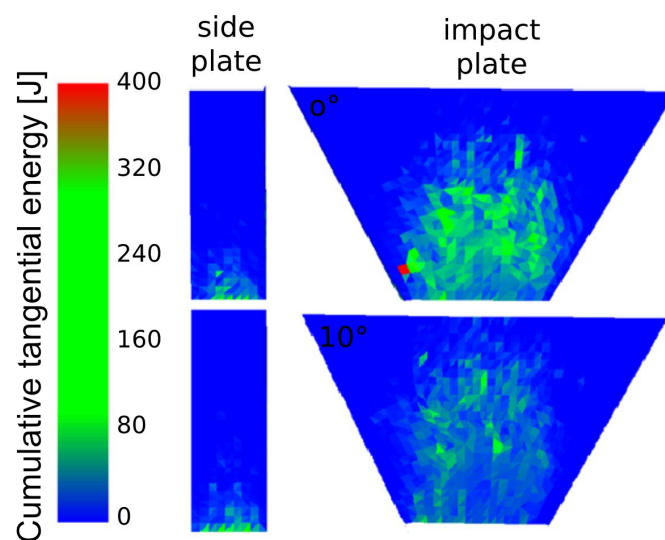


**Figure 13.** Cumulated tangential energy after 60 s of simulation for the impact plate and the side plate mounted vertically and at an angle of  $10^\circ$  of the structure, for 900 Mg/h.

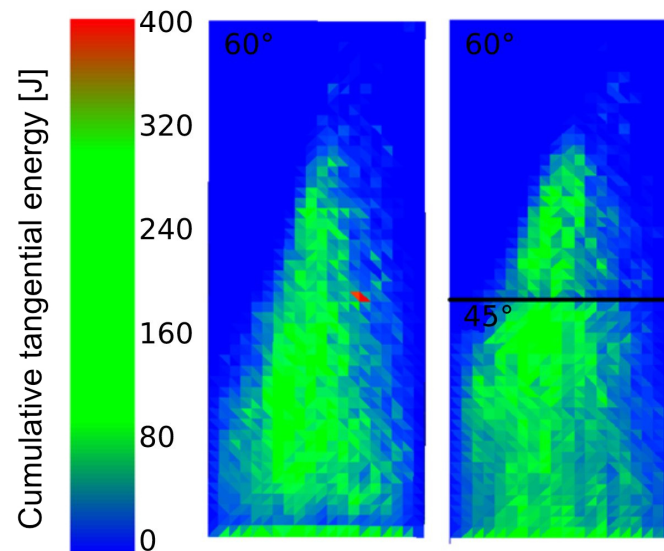


**Figure 14.** Cumulated tangential energy after 60 s of simulation on the chute, for 900 Mg/h.

#### 4.4. Implementation of the New Design

The variant with an inclined impact plate and a chute with two parts of different inclination was chosen as the best and simplest solution. This design of the transfer station has been implemented (Figure 15a) in the mining plant and successfully fulfills its task (Figure 15b). The elements of the transfer station were reinforced with abrasion-resistant steel, which will ensure the long life of these elements. The elimination of the risk of blockages and the positioning of the spoil stream centrally on the receiving conveyor demonstrate the suitability of the granite DEM model for optimization activities.

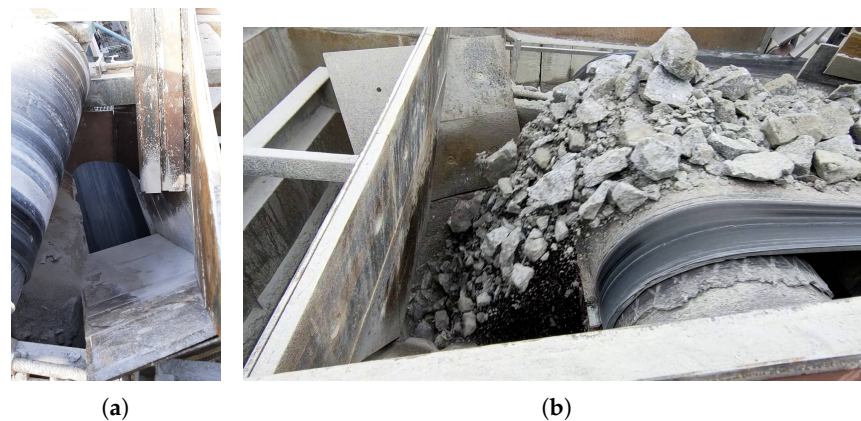


**Figure 15.** New transfer station: (a) prepared, and (b) in operation.

## 5. Discussion and Conclusions

For the purpose of this research, a laser scan was performed of the existing transfer station in the “Graniczna” mine, between the WD-1 and the B-1 conveyors. A CAD model for the DEM simulation was developed from the obtained point cloud using reverse engineering methods. Nominal capacities of the conveyors were determined with allowance for their parameters. Examinations included the material parameters of granite and the coefficients of friction against steel and rubber. The remaining parameters were calibrated against the flow time and the angle of repose in the calibration box. Then, the normal operating conditions of the transfer station were mapped in the simulation, subsequently involving the potential unfavorable conditions. The results of the simulations allowed the design defects of the current construction to be determined.

An alternative transfer station in the form of an impact plate and a chute was proposed. The energy lost by the aggregate stream on the belt and on the transfer station elements was also determined for the proposed variants. Cumulative energy lost on the chute and on the belt by the material stream was chosen as an optimization criterion. The quarry staff implemented the proposed design solution in the analyzed transfer point. The transfer station fulfilled the tasks set for it and contributed to reducing the failure rate of the conveyor belt.

The most important conclusions from the conducted analysis are as follows:

- The receiving conveyor is inclined at a large angle, and the temporary capacities exceed its theoretical nominal capacity, which may lead to unfavorable phenomena. Regardless of the transfer station design, if the material stream capacity is greater than the nominal capacity of the receiving conveyor, a failure may occur.
- The previous design of the station was sufficient when the material was dry, and the grain distribution was in accordance with the one presented in Figure 3.
- When unfavorable factors coincide, i.e., the percentage of large solids increases, the temporary capacity increases in wet conditions, and an arch may be formed, blocking the discharge space at a temporary capacity of approximately 600 Mg/h.
- The functionality of the transfer station was improved by installing elements that ensure continuous transport of the material without accumulating the material on the shelves.
- The station, which consists of an impact plate and a chute, allows for a failure-free transfer of aggregate material in difficult operating conditions.
- The use of a chute installed at an angle of 45° reduced the energy lost by the material on the belt by more than 10 percent.
- The impact plate, inclined at an angle of 10°, is characterized by lower wear than the vertical variant.

**Author Contributions:** Conceptualization, B.D. and R.K.; methodology, B.D.; software, B.D. and J.W.; validation, B.D.; formal analysis, B.D.; investigation, B.D.; resources, B.D., J.W. and R.K.; data curation, B.D. and J.W.; writing—original draft preparation, B.D.; writing—review and editing, R.K. and J.W.; visualization, B.D.; supervision, R.K.; project administration, R.K.; funding acquisition, R.K. All authors have read and agreed to the published version of the manuscript.

**Funding:** The research work was co-funded with the research subsidy of the Polish Ministry of Science and Higher Education granted for 2021.

**Institutional Review Board Statement:** Not applicable.

**Informed Consent Statement:** Not applicable.

**Data Availability Statement:** The data presented in this study are available on request from the corresponding author.

**Acknowledgments:** We want to acknowledge cooperation with the “Graniczna” quarry from EU-ROVIA KRUSZYWA S.A. The quarry management provided us with objects to analyze and handled the project implementation and tests.

**Conflicts of Interest:** The authors declare no conflict of interest.

## References

1. Czuba, W.; Furmanik, K. Analiza ruchu ziarna w przestrzeni przesykowej przenośnika taśmowego. *Ekspluat. I Niezawodn.* **2013**, *15*, 390–396.
2. Roberts, A.; Arnold, P. Discharge—Chute design for free—Flowing granular materials. *Trans. Am. Soc. Agric. Eng.* **1971**, *14*. [[CrossRef](#)]
3. Rudolf, L.; Durna, A.; Hapla, T. The issue of the transfer points on belt conveyors. *Int. Multidiscip. Sci. GeoConf. Surv. Geol. Min. Ecol. Manag. SGEM* **2018**, *18*, 989–996. [[CrossRef](#)]
4. Grincova, A.; Andrejiova, M.; Marasova, D.; Khouri, S. Measurement and determination of the absorbed impact energy for conveyor belts of various structures under impact loading. *Meas. J. Int. Meas. Confed.* **2019**, *131*, 362–371. [[CrossRef](#)]



5. Fedorko, G.; Molnar, V.; Marasova, D.; Grincova, A.; Dovica, M.; Zivcak, J.; Toth, T.; Husakova, N. Failure analysis of belt conveyor damage caused by the falling material. Part I: Experimental measurements and regression models. *Eng. Fail. Anal.* **2014**, *36*, 30–38. [[CrossRef](#)]
6. L'ubomír, A.; Taraba, V.; Szabo, S.; Leco, M. Belt damage aspect to impact loading. *Appl. Mech. Mater.* **2014**, *683*, 102–107. [[CrossRef](#)]
7. Gutierrez, A.; Garate, G. Design of a transfer chute for multiple operating conditions. *ASME Int. Mech. Eng. Congr. Expo. Proc. (IMECE)* **2014**, *11*. [[CrossRef](#)]
8. Hastie, D.B.; Wypych, P.W. Experimental validation of particle flow through conveyor transfer hoods via continuum and discrete element methods. *Mech. Mater.* **2010**, *42*, 383–394. [[CrossRef](#)]
9. Ilic, D.; Roberts, A.; Wheeler, C.; Katterfeld, A. Modelling bulk solid flow interactions in transfer chutes: Shearing flow. *Powder Technol.* **2019**, *354*, 30–44. [[CrossRef](#)]
10. Katterfeld, A.; Wensrich, C. Understanding granular media: From fundamentals and simulations to industrial application. *Granul. Matter* **2017**, *19*. [[CrossRef](#)]
11. Gröger, T.; Katterfeld, A. Application of the discrete element method in materials handling—Part 3: Transfer stations. *Bulk Solids Handl.* **2007**, *27*, 158–166.
12. Nordell, L.K. Palabora installs curved transfer chute in hard rock to minimize belt cover wear. *Bulk Solids Handl.* **1994**, *14*, 739–743.
13. Rossow, J.; Coetzee, C. Discrete element modelling of a chevron patterned conveyor belt and a transfer chute. *Powder Technol.* **2021**, *391*, 77–96. [[CrossRef](#)]
14. Ilic, D.; Lavrinec, A.; Orozovic, O. Simulation and analysis of blending in a conveyor transfer system. *Miner. Eng.* **2020**, *157*, 106575. [[CrossRef](#)]
15. Xu, Z.; Xu, E.; Wu, L.; Liu, S.; Mao, Y. Registration of terrestrial laser scanning surveys using terrain-invariant regions for measuring exploitative volumes over open-pit mines. *Remote Sens.* **2019**, *11*, 606. [[CrossRef](#)]
16. Bazarnik, M. Slope stability monitoring in open pit mines using 3D terrestrial laser scanning. In *E3S Web of Conferences*; EDP Sciences: Julis, France, 2018; Volume 66, p. 01020.
17. Vassena, G.; Clerici, A. Open pit mine 3D mapping by tls and digital photogrammetry: 3D model update thanks to a slam based approach. *Int. Arch. Photogramm. Remote Sens. Spat. Inf. Sci.* **2018**, *42*, 1145–1148. [[CrossRef](#)]
18. Yang, H.; Xu, X.; Neumann, I. Laser scanning-based updating of a finite-element model for structural health monitoring. *IEEE Sens. J.* **2015**, *16*, 2100–2104. [[CrossRef](#)]
19. Skoczylas, A.; Kamoda, J.; Zaczek-Peplinska, J. Geodetic monitoring (TLS) of a steel transport trestle bridge located in an active mining exploitation site. *Ann. Wars. Univ. Life Sci. Sggw. Land Reclam.* **2016**, *48*, 255–266. [[CrossRef](#)]
20. Lipecki, T.; Kim, T.T.H. The Development of Terrestrial Laser Scanning Technology and Its Applications in Mine Shafts in Poland. *Inżynieria Miner.* **2020**, *1*, 301–310.
21. Fengyun, G.; Hongquan, X. Status and development trend of 3D laser scanning technology in the mining field. In *2013 the International Conference on Remote Sensing, Environment and Transportation Engineering (RSETE 2013)*; Atlantis Press: Nanjing, China, 2013.
22. Fojtík, D. Measurement of the volume of material on the conveyor belt measuring of the volume of wood chips during transport on the conveyor belt using a laser scanning. In Proceedings of the 2014 15th International Carpathian Control Conference (ICCC), Velke Karlovice, Czech Republic, 28–30 May 2014; pp. 121–124.
23. Trybała, P.; Blachowski, J.; Błażej, R.; Zimroz, R. Damage Detection Based on 3D Point Cloud Data Processing from Laser Scanning of Conveyor Belt Surface. *Remote Sens.* **2021**, *13*, 55. [[CrossRef](#)]
24. Roberts, A.W. An Investigation of the Gravity Flow of Noncohesive Granular Materials Through Discharge Chutes. *J. Manuf. Sci. Eng. Trans. ASME* **1969**, *91*, 373–381. [[CrossRef](#)]
25. Kruczek, P.; Polak, M.; Wyłomańska, A.; Kawalec, W.; Zimroz, R. Application of compound Poisson process for modelling of ore flow in a belt conveyor system with cyclic loading. *Int. J. Min. Reclam. Environ.* **2018**, *32*, 376–391. [[CrossRef](#)]
26. Gładysiewicz, L. *Przenośniki Taśmowe Teoria i Obliczenia*; Oficyna Wydawnicza Politechniki Wrocławskiej: Wrocław, Poland, 2003.
27. Grima, A.P.; Wypych, P.W. Investigation into calibration of discrete element model parameters for scale-up and validation of particle-structure interactions under impact conditions. *Powder Technol.* **2011**, *212*, 198–209. [[CrossRef](#)]
28. Doroszuk, B.; Król, R. Analysis of conveyor belt wear caused by material acceleration in transfer stations. *Min. Sci.* **2019**, *26*, 189–201. [[CrossRef](#)]
29. Walker, P.; Doroszuk, B.; Król, R. Analysis of ore flow through longitudinal belt conveyor transfer point. *Ekspluat. I Niezawodn.* **2020**, *22*, 536–543. [[CrossRef](#)]
30. Roessler, T.; Richter, C.; Katterfeld, A.; Will, F. Development of a standard calibration procedure for the DEM parameters of cohesionless bulk materials—Part I: Solving the problem of ambiguous parameter combinations. *Powder Technol.* **2019**, *343*, 803–812. [[CrossRef](#)]
31. Persson, B.N.J.; Tartaglino, U.; Albohr, O.; Tosatti, E. Rubber friction on wet and dry road surfaces: The sealing effect. *Phys. Rev.* **2005**, *71*. [[CrossRef](#)]
32. Roberts, A.W. *Characterisation for Hopper and Stockpile Design*; Blackwell Publishing Ltd.: Hoboken, NJ, USA, 2009; pp. 85–131. [[CrossRef](#)]
33. Kessler, F.; Prenner, M. DEM—Simulation of conveyor transfer chutes. *FME Trans.* **2009**, *37*, 185–192.
34. Roberts, A.W. Chute performance and design for rapid flow conditions. *Chem. Eng. Technol.* **2003**, *26*, 163–170. [[CrossRef](#)]